

# Quantum quench in 1D: Coherent inhomogeneity amplification and ‘supersolitons’

Matthew S. Foster\* and Emil A. Yuzbashyan  
*Center for Materials Theory, Department of Physics and Astronomy,  
 Rutgers University, Piscataway, NJ 08854, USA*

Boris L. Altshuler  
*Physics Department, Columbia University, New York, NY 10027, USA*  
 (Dated: October 11, 2018)

We study a quantum quench in a 1D system possessing Luttinger liquid (LL) and Mott insulating ground states before and after the quench, respectively. We show that the quench induces power law amplification in time of any particle density inhomogeneity in the initial LL ground state. The scaling exponent is set by the fractionalization of the LL quasiparticle number relative to the insulator. As an illustration, we consider the traveling density waves launched from an initial localized density bump. While these waves exhibit a particular rigid shape, their amplitudes grow without bound.

PACS numbers:

The shattering of cold glass in hot water is but one of many spectacular effects that can be induced by a rapid thermal quench in classical media. What happens when an isolated *quantum* phase of matter is subject to a sudden, violent deformation of its system Hamiltonian (a ‘quantum quench’)? This question is now under vigorous investigation in cold atomic gases [1–4]. Long-time, out-of-equilibrium physics already observed in gases confined to one [2], two [3], and three [4] spatial dimensions includes oscillatory collapse and revival phenomena [2, 4] and topological defect formation [3, 5].

In this Letter, we study interaction quenches in one-dimensional (1D) quantum many body systems. Prior theory assuming spatially uniform dynamics has considered the post-quench distribution of quasiparticles [6], correlation functions [7, 8], thermalization [6, 9], quantum critical scaling [10], etc. On the other hand, the stability of homogeneous solutions with respect to the spontaneous eruption of spatial non-uniformity is by no means guaranteed, due to the coupling between modes with different momenta and the extensive quantity of energy injected into the system by the quench. Indeed, homogeneous external perturbations are known to generate large spatial modulations in a variety of physical contexts [5, 11]. We show here that quantum quenches can produce strongly inhomogeneous states via a mechanism that is ubiquitous in 1D.

We consider quenches across a quantum critical point, with initial (pre-) and final (post-quench) Hamiltonians possessing Luttinger liquid (LL) and Mott insulator ground states, respectively. Specifically, we quench into the insulating phase of the quantum sine Gordon model at the ‘Luther-Emery’ (LE) point [8, 10, 12–14], where we are able to determine the dynamics analytically. The pre-quench ground state has an inhomogeneous density profile  $\rho_0(x)$ , which acts as a ‘seed’ generating fluctuations in the space-time dynamics of local observables [15, 16]. We find that an arbitrarily small deviation of

$\rho_0(x)$  from a constant is dynamically amplified by the time evolution, see e.g. Figs. 1 and 2. We argue that the mechanism responsible for the amplification is quasiparticle *fractionalization*, a generic attribute of gapless interacting particles in 1D [12, 17]. We further illustrate the amplification effect for a localized (Gaussian) initial density ‘bump.’ This bump gives rise to a pair of non-dispersive, non-interacting density waves that exhibit a rigid shape, with amplitudes that grow in time as a power law. We have dubbed these traveling density waves ‘supersolitons’; an example is depicted in Fig. 2.

Specifically, for the Fourier transform  $\tilde{\rho}(t, k)$  of the density operator expectation value  $\rho(t, x)$ , we find the following exact asymptotic result, valid in the long time limit:

$$\frac{\tilde{\rho}(t, k)}{\tilde{\rho}_0(k)} = \cos(kt') - \mathcal{A}_\sigma (|k|t')^{\sigma/2} \cos\left(|k|t' + \frac{\pi\sigma}{4}\right), \quad (1)$$

where  $\mathcal{A}_\sigma$  is a non-universal,  $k$ -independent constant and

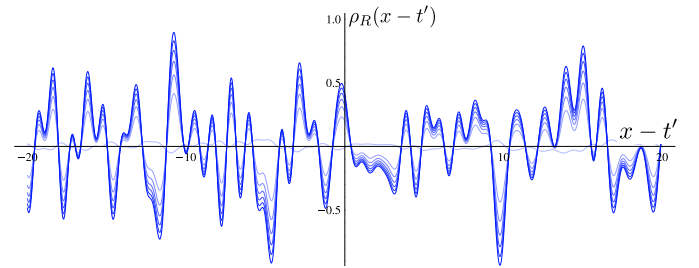


FIG. 1: Space-time evolution of the right-moving number density  $\rho_R$  after Luttinger liquid to Mott insulator quench, demonstrating the instability of spatially uniform dynamics; fainter (bolder) traces depict earlier (later) times. An infinitesimally small initial density inhomogeneity grows without bound. The figure is obtained from Eq. (1) with  $\sigma = 0.8$ ,  $\mathcal{A}_\sigma = 4.7$ , and an initial density profile  $\rho_0(x)$  given by a sum of 150 cosines with random amplitudes, phases, and wavenumbers. Amplification occurs for any non-zero  $\sigma$ , corresponding to a non-zero fractionalization of the initial LL quasiparticles with respect to the insulator.

$t' \equiv t/\bar{K}$ , where  $\bar{K} = 1/4$  locates the LE point (see below); the quench is performed at  $t' = 0$ . The exponent  $\sigma$  in Eq. (1) is determined by the relative fractionalization of the LL quasiparticle number with respect to the Mott insulator,

$$\sigma \equiv (\bar{K}/2K + K/2\bar{K}) - 1, \quad (2)$$

where  $K$  is the Luttinger parameter characterizing the initial Hamiltonian. Eq. (1) implies that the density splits into non-dispersing left- and right-moving components,  $\rho(t, x) = \rho_R(x - t') + \rho_L(x + t')$ . Interestingly, the long time response is linear in  $\tilde{\rho}_0$  and enhanced at shorter wavelengths due to the fractional derivative ( $|k|^{\sigma/2}$ ) factor. For  $\sigma > 0$ , the fluctuations of  $\rho_{R,L}$  are continuously amplified by the quench. The effect is demonstrated in Fig. 1

In the rest of this Letter, we will explain the setup and calculations leading to Eq. (1). Before the quench, our cold atom system is assumed to reside in the ground state  $|0\rangle_{\rho_0}$  of the LL Hamiltonian

$$H_i = \int dx \left[ \frac{vK}{2} \left( \frac{d\hat{\phi}}{dx} \right)^2 + \frac{v}{2K} \left( \frac{d\hat{\theta}}{dx} \right)^2 - \frac{\rho_0(x)}{q\sqrt{\pi}} \frac{d\hat{\theta}}{dx} \right], \quad (3)$$

where  $v$  is the sound velocity,  $K$  is the Luttinger parameter, and  $\rho_0(x)/q$  is an external chemical potential, with  $q \equiv K/v\pi$ . The Hamiltonian in Eq. (3) governs the low-energy, long-wavelength physics of many gapless 1D cold atomic and condensed matter quantum systems [12, 18]; in this paper, we have in mind a 1D optical lattice gas of spin-polarized, neutral Fermi atoms, but other interpretations are possible. The short-ranged interatomic interactions determine  $v$  and  $K$ ; repulsive (attractive) interactions correspond to  $K < 1$  ( $K > 1$ ), while the free Fermi gas has  $K = 1$  and  $v$  equal to the bare Fermi velocity. The boson fields  $\hat{\phi}$  and  $\hat{\theta}$  encode fluctuations of the long wavelength fermion number density  $:\hat{\rho}:$  and current  $:\hat{J}:$  on top of the filled Fermi sea via  $\sqrt{\pi}:\hat{\rho}:=d\hat{\theta}/dx$  and  $\sqrt{\pi}:\hat{J}:=d\hat{\phi}/dx$ , where  $:\dots:$  denotes normal-ordering with respect to the *homogeneous* ground state  $|0\rangle_{\rho_0=0}$ . These satisfy the commutation relations  $[:\hat{\rho}(x):, :\hat{J}(x'):] = -(i/\pi)(d/dx)\delta(x - x')$ . The static chemical potential in Eq. (3) allows us to “write” an arbitrary density profile into  $|0\rangle_{\rho_0}$  via the axial anomaly [12, 19],

$$\rho_0 \langle 0 | :\hat{\rho}(x): | 0 \rangle_{\rho_0} = \rho_0(x), \quad \rho_0 \langle 0 | :\hat{J}(x): | 0 \rangle_{\rho_0} = 0. \quad (4)$$

With our system initially prepared in the LL ground state  $|0\rangle_{\rho_0}$ , we perform the quench at time  $t = 0$ . The dynamics for  $t > 0$  are generated by the translationally invariant, “final state” Hamiltonian  $H_f$ , which favors a gapped, Mott insulating ground state. Specifically,  $H_f$  is

the Hamiltonian of the quantum sine Gordon model,

$$H_f = \frac{1}{K_f} \int dx \left[ \frac{1}{2} \left( \frac{d\hat{\Phi}}{dx} \right)^2 + \frac{1}{2} \left( \frac{d\hat{\Theta}}{dx} \right)^2 + \frac{M}{\pi\alpha} \cos \left( 2\sqrt{4\pi K_f} \hat{\Theta} \right) \right]. \quad (5)$$

In Eq. (5) we have expressed  $H_f$  in terms of the canonically rescaled boson variables  $\hat{\Phi} \equiv \sqrt{K_f} \hat{\phi}$  and  $\hat{\Theta} \equiv \hat{\theta}/\sqrt{K_f}$ . The Mott gap-inducing interparticle interactions set the parameters  $M$  and  $K_f$ . In the context of a Fermi lattice gas at commensurate filling, the “Luttinger parameter”  $K_f$  characterizes pure forward scattering, while  $M$  gives the strength of backward scattering Umklapp interactions;  $\alpha$  is a cutoff-dependent length scale. The ground state of  $H_f$  is gapped for arbitrarily small  $M$  over the regime  $0 < K_f < 1/2$ , in which the quantum sine Gordon model is integrable [12]. The solitons and antisolitons of the classical sine Gordon equation appear as massive Dirac fermions in the quantum version [20]. Solitons repel antisolitons for  $1/4 < K_f < 1/2$  and attract them for  $0 < K_f < 1/4$ ; in the latter case, additional bosonic bound states (*breathers*) appear in the spectrum. We choose to quench to the boundary between these two regimes, where  $K_f = \bar{K} \equiv 1/4$ . At this special “Luther-Emery” point, the interactions between the quantum solitons switch off, and  $H_f$  can be *re-fermionized* [14] in terms of a massive non-interacting soliton field  $\Psi$ ,

$$H_f = \frac{1}{K} \int dx \Psi^\dagger \left( -i\hat{\sigma}^3 \frac{d}{dx} + \bar{M}\hat{\sigma}^2 \right) \Psi. \quad (6)$$

In this equation,  $\Psi$  is a two-component Dirac fermion that is related to the boson fields in Eq. (5) via the bosonization identity,  $\Psi^{(1,2)} \propto \exp[i\sqrt{\pi}(\hat{\Phi} \pm \hat{\Theta})]$ ;  $\hat{\sigma}^{2,3}$  are Pauli matrices in the standard basis. The mass gap  $\bar{M}$  in Eq. (6) is a non-universal, cutoff-dependent quantity.

It is instructive to rewrite  $H_i$  [Eq. (3)] in terms of  $\Psi$ ,

$$H_i = \int dx \left\{ \tilde{v}\Psi^\dagger \left( -i\hat{\sigma}^3 \frac{d}{dx} \right) \Psi - \frac{\rho_0(x)}{2q} \Psi^\dagger \Psi + \frac{\pi\tilde{v}}{2K^2} [\bar{K}^2 - K^2] : \Psi^\dagger \Psi :: \Psi^\dagger \Psi : \right\}, \quad (7)$$

where  $\tilde{v} \equiv Kv/\bar{K}$ . Comparing Eqs. (6) and (7), we see that the quench with  $K = \bar{K}$  is special. For this case only (“non-interacting” quench), the quasiparticles of the initial and final Hamiltonians are in one-to-one correspondence. At any other value of  $K \neq \bar{K}$  (“interacting quench”), an elementary excitation of the initial state carries a fraction of the final state quasiparticle number; that is, the “quasiparticle” excitations of the initial LL phase carry  $K/\bar{K} = 4K$  of the global  $U(1)$   $\Psi$  fermion number charge [17]. When viewed in terms of  $\Psi$ , the transition between  $H_i$  and  $H_f$  permits a dual interpretation as a LL to band insulator quench. Correlation

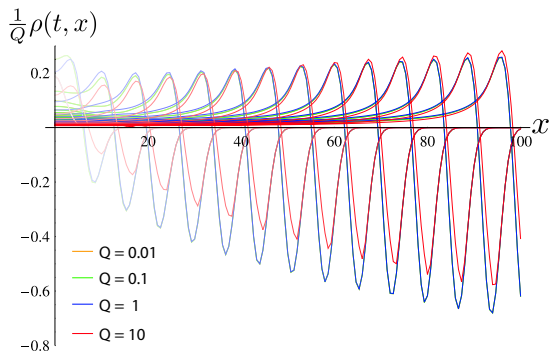


FIG. 2: The right-moving ‘supersoliton.’ The number density evolution after Luttinger liquid to Mott insulator quench is depicted as in Fig. 1, but here for a Gaussian initial profile  $\sqrt{\pi}\Delta\rho_0(x) = Q \exp(-x^2/\Delta^2)$ , with  $\sigma = 0.7$ , now obtained via numerical integration of the exact bosonization result [21]. Time series for four different  $Q$  are plotted; the densities are normalized relative to these. The evolution is reflection symmetric about  $x = 0$ .

functions in the homogeneous quench [ $\rho_0(x) = 0$ ] have been previously studied in Refs. [8, 13].

To characterize the post-quench dynamics, we compute the expectation values of the particle number ( $\rho$ ), kinetic ( $\mathcal{K}$ ) and potential ( $\mathcal{U}$ ) energy densities (the latter two observables are defined with respect to  $H_f$ ):

$$\rho(t, x) = \frac{1}{2} \rho_0 \langle 0 | \Psi^\dagger(t, x) \Psi(t, x) | 0 \rangle_{\rho_0}, \quad (8a)$$

$$\mathcal{K}(t, x) \equiv -\frac{i}{2} \rho_0 \langle 0 | \Psi^\dagger(t, x) \hat{\sigma}^3 \overleftrightarrow{\partial}_x \Psi(t, x) | 0 \rangle_{\rho_0}, \quad (8b)$$

$$\mathcal{U}(t, x) \equiv \rho_0 \langle 0 | \Psi^\dagger(t, x) \hat{\sigma}^2 \Psi(t, x) | 0 \rangle_{\rho_0}, \quad (8c)$$

where  $f \overleftrightarrow{\partial} g \equiv f \partial g - (\partial f) g$ . In these equations,  $\Psi(t, x)$  denotes the Heisenberg picture fermion operator whose dynamics are generated by  $H_f$  in Eq. (6).  $\mathcal{U}$  gives the expectation of the cosine operator in the sine Gordon model [Eq. (5)], and can be interpreted as a (squared) order parameter for the Mott phase. We obtain  $\rho$ ,  $\mathcal{K}$ , and  $\mathcal{U}$  by solving the Heisenberg equations of motion for  $\Psi(t, x)$  and exploiting the bosonization map. Given an arbitrary initial  $\rho_0(x)$ , we have derived exact results for  $\rho$ ,  $\mathcal{K}$ , and  $\mathcal{U}$  at any time  $t \geq 0$ , which will appear elsewhere [21].

The exact post-quench observables in Eq. (8) depend upon  $\rho_0(x)$ ,  $\bar{M}$ , and the dynamic exponent  $\sigma$  defined via Eq. (2). The non-interacting quench with  $K = \bar{K}$  has  $\sigma = 0$ , while the interacting quench ( $K \neq \bar{K}$ ) has  $\sigma > 0$ . We confine ourselves to the range  $0 \leq \sigma < 1$ , for which the  $\rho_0(x)$ -dependent contributions to  $\rho$ ,  $\mathcal{K}$ , and  $\mathcal{U}$  are given by ultraviolet (UV) convergent integrals [21]. At  $\sigma = 1$ , these observables acquire logarithmic UV divergences, suggesting the onset of a sensitive dependence on lattice scale details.

We now describe our main results, which concern the  $\rho_0(x)$ -dependent contributions to  $\rho$ ,  $\mathcal{K}$ , and  $\mathcal{U}$ ; the be-

havior of  $\mathcal{K}$  and  $\mathcal{U}$  for the homogeneous quench  $\rho_0 = \rho(t, x) = 0$  will be discussed elsewhere [21]. The exact leading asymptotic expression for  $\rho(t, x)$  in the limit  $t \rightarrow \infty$  was already given by Eq. (1), above. Let us specialize this result to a localized initial density profile. The interacting ( $\sigma > 0$ ) versus non-interacting ( $\sigma = 0$ ) quenches yield qualitatively different behaviors. For the interacting quench, Eq. (1) implies that  $\rho(t, x)$  develops a non-dispersive response to the initial condition for any  $0 < \sigma < 1$ . For example, a Gaussian density bump,  $\sqrt{\pi}\Delta\rho_0(x) = Q \exp(-x^2/\Delta^2)$ , induces the following asymptotic space-time evolution for  $t \gg 1/\bar{M}$ :

$$\begin{aligned} \rho(t, x) = & \frac{Q}{2\sqrt{\pi}\Delta} e^{-\frac{(x-t')^2}{\Delta^2}} \\ & - \frac{Q}{2\Delta} \frac{\Gamma(1-\sigma)}{\Gamma(\frac{1+\sigma}{2})} \left[ \frac{(K\bar{M}\alpha)^2 t'}{\sqrt{2}\Delta} \right]^{\sigma/2} \\ & \times e^{-\frac{(x-t')^2}{2\Delta^2}} D_{\sigma/2} \left[ \sqrt{2} \left( \frac{x-t'}{\Delta} \right) \right] \\ & + \{x \rightarrow -x\}, \end{aligned} \quad (9)$$

where  $D_\nu(x)$  denotes the parabolic cylinder function,  $t' = t/\bar{K}$ , and we have written out the explicit form of the prefactor  $\mathcal{A}_\sigma$ , which is non-universal for  $\sigma > 0$  and depends upon  $\bar{M}\alpha$ . The naive continuum calculation gives  $\bar{M}\alpha = 15/16$ . The divergence of the prefactor at  $\sigma = 1$  indicates the onset of sensitivity to the UV sector of the theory.

Eq. (9) implies that an antecedent Gaussian density bump splits into right- and left-moving non-dispersive waves, for generic  $Q$ ,  $\Delta$ , and  $K \neq \bar{K}$  ( $\sigma > 0$ ). In the long time limit, the leading response is *strictly linear* in  $Q$ , with an amplitude that grows as  $t'^{\sigma/2}$ . Two Gaussian bumps initially separated by a distance  $d \gg \Delta$  can be used to create left- and right-moving waves which pass through each other without changing their form [21]. We dub these rigid, non-interacting density waves ‘supersolitons’ to distinguish them from the elementary quantum solitons annihilated by the fermion field  $\Psi$ . We have confirmed the asymptotic result in Eq. (9) by comparing to numerical integration of the exact bosonization expression for  $\rho$ . The supersoliton is exhibited in Fig. 2.

Although the precise shape of the supersoliton implied by Eq. (9) deforms continuously with  $\sigma$ , it exhibits the same positive-negative ‘dipolar’ peak profile for any  $0 < \sigma < 1$  (see Fig. 2). The negative density dip represents a local evacuation of the filled Fermi sea, which is infinitely deep in the Luttinger model [12]. For any  $\sigma > 0$ , the integral of the second term in Eq. (9) over real  $x$  vanishes, consistent with particle number conservation. In the limit of the non-interacting quench  $\sigma \rightarrow 0$ , the right-hand side of Eq. (9) vanishes; in this case, the response obtains entirely from subleading terms that do not grow with  $t$  (and conserve the particle number), but which we have not written here. The same is true in

Eq. (1) because  $\mathcal{A}_\sigma \rightarrow 1$  when  $\sigma \rightarrow 0$ .

For comparison, Fig. 3 depicts the number density  $\rho(t, x)$  for the case  $\sigma = 0$ , obtained by numerical integration of the exact result. The main message of this figure is that the non-interacting post-quench dynamics are “passive” and dispersive, depending sensitively upon the details of the initial inhomogeneity and showing no amplification phenomena.

In the interacting quench, the supersoliton is also observed in the relative kinetic energy density, defined as  $\delta\mathcal{K}[t, x; \rho_0] \equiv \mathcal{K}[t, x; \rho_0] - \mathcal{K}[t, x; 0]$ , shown in Fig. 4. By contrast, we find that the potential energy density  $\mathcal{U}(t, x)$  does not exhibit the supersoliton on top of the homogeneous background it acquires after the quench. The amplification in Eq. (1) does not therefore appear related to a Kibble-Zurek process [5] in the order parameter.

The physical mechanism underlying the power law inhomogeneity growth in Eqs. (1) and (9) can be partially elucidated via an analogy to the equilibrium tunneling density of states (TDOS)  $\nu(\omega)$  in a LL [17]. Upon tunneling into a one channel quantum wire at  $T = 0$  characterized by the Luttinger parameter  $K$ , the conductance at a bias  $\omega = eV$  diminishes as  $\nu(\omega) \sim |\omega|^\sigma$  where  $\sigma$  is defined as in Eq. (2), but with  $\bar{K} = 1$ . The physics behind this result is a follows: The independent LL “quasiparticles” carry a fraction  $K$  of the electron charge  $e$  [17]. The TDOS  $\nu(\omega)$  vanishes as  $\omega \rightarrow 0$  because a “whole” electron must fractionalize into a large number of pieces upon penetrating into the LL, and this process is prohibited by phase space restrictions in the low bias limit. Mathematically, the TDOS result obtains from the Fourier transform of the electron Green’s function in the LL. The  $t^{\sigma/2}$  amplification in Eq. (1) is rendered by a similar mechanism in the quench: an initial LL correlation function is convolved with an oscillatory kernel [a product of Green’s functions resulting from the solution to the Heisenberg

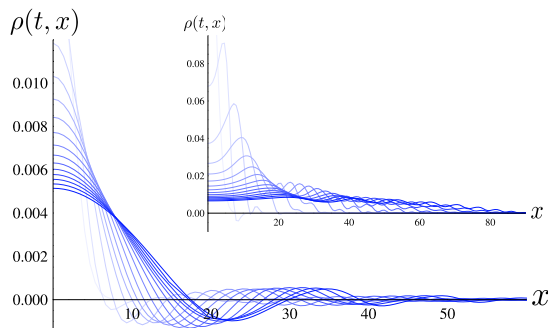


FIG. 3: The number density evolution as in Fig. 2, but for the non-interacting quench  $K = \bar{K}$  ( $\sigma = 0$ ). The height of the initial bump is  $Q = 0.1$  in the main figure and  $Q = 1$  in the inset; the evolution is reflection symmetric about  $x = 0$ . Now there is no fractionalization of the initial LL quasiparticles with respect to the insulator and, consequently, the dynamics are simply dispersive with no supersolitons or inhomogeneity growth.

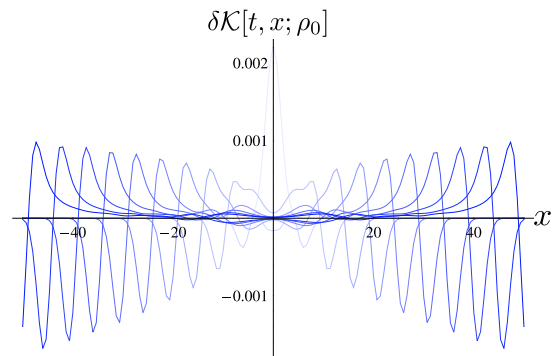


FIG. 4: The kinetic energy density supersolitons. This figure depicts the post-quench space-time evolution of the relative kinetic energy density expectation value  $\delta\mathcal{K}[t, x; \rho_0]$  (see text) for  $K = 0.77 \neq \bar{K}$  and an initial Gaussian density bump.

equations of motion for  $\Psi(t, x)$ . The final state Hamiltonian  $H_f$  introduces a scale  $\bar{M}$ , by which the analog of the frequency  $\omega$  in the TDOS is the evolution interval  $\bar{M}^2 t$ . We might therefore naively expect  $\rho(t, x) \sim t^\sigma$ , with  $\sigma$  defined by Eq. (2). That the leading power is  $\sigma/2$  in Eqs. (1) and (9) obtains from a cancelation of  $t^\sigma$  terms. This suggests that the *immiscibility* of quantum phases composed of quasiparticles carrying relatively fractional charges may underlie both the equilibrium TDOS and the quench amplification.

In conclusion, we have shown that a quantum quench can beget a strongly inhomogeneous state, due to the interplay between quasiparticle fractionalization and the presence of a mass scale in the final state Hamiltonian. Fractionalization is a robust feature of 1D gapless phases, so we expect the inhomogeneity proliferation to occur in many 1D quantum quenches. It would be interesting to consider quenches to final states away from the free fermion LE point where (super?) soliton-soliton interactions can play a role in the dynamics.

We would like to thank Leon Balents for helpful discussions of LL physics. This work was supported by the National Science Foundation under Award No. DMR-0547769 and by the David and Lucille Packard Foundation.

\* Electronic address: psiborf@rci.rutgers.edu

- [1] I. Bloch, J. Dalibard, and W. Zwerger, *Rev. Mod. Phys.* **80**, 885 (2008).
- [2] T. Kinoshita, T. Wenger, and D. S. Weiss, *Nature (London)* **440**, 900 (2006).
- [3] L. E. Sadler *et al.*, *Nature (London)* **443**, 312 (2006).
- [4] M. Greiner *et al.*, *Nature (London)* **419**, 51 (2002).
- [5] T. W. B. Kibble, *J. Phys. A* **9**, 1387 (1976); W. H. Zurek, *Nature (London)* **317**, 505 (1985).
- [6] M. Rigol *et al.*, *Phys. Rev. Lett.* **98**, 050405 (2007); M. Rigol, V. Dunjko, and M. Olshanii, *Nature (London)*

- 452**, 854 (2008).
- [7] P. Calabrese and J. Cardy, Phys. Rev. Lett. **96**, 136801 (2006); J. Stat. Mech. P06008 (2007).
- [8] V. Gritsev *et al.*, Phys. Rev. Lett. **99**, 200404 (2007).
- [9] D. Rossini *et al.*, Phys. Rev. Lett. **102**, 127204 (2009); arXiv: 1002.2842.
- [10] C. De Grandi, V. Gritsev, and A. Polkovnikov, Phys. Rev. B **81**, 012303 (2010); arXiv: 0910.0876.
- [11] M. Dzero, E. A. Yuzbashyan, and B. L. Altshuler, Europhys. Lett. **85**, 20004 (2009).
- [12] For a review, see e.g. A. O. Gogolin, A. A. Nersisyan, and A. M. Tsvelik, *Bosonization and Strongly Correlated Systems* (Cambridge University Press, Cambridge, 1998).
- [13] A. Iucci and M. A. Cazalilla, arXiv: 1003.5167.
- [14] A. Luther and V. J. Emery, Phys. Rev. Lett. **33**, 589 (1974).
- [15] J. Mossel and J.-S. Caux, arXiv: 1002.3988.
- [16] J. Lancaster and A. Mitra, arXiv: 1002.4446.
- [17] For a review, see M. P. A. Fisher and L. I. Glazman, in *Mesoscopic Electron Transport*, edited by Sohn, Kouwenhoven, and Schön (Kluwer, The Netherlands, 1997).
- [18] M. A. Cazalilla, J. Phys. B **37**, S1 (2004).
- [19] Due to the strictly linear spectrum assumed in the Luttinger model, the scalar potential does not confine or localize the liquid, but merely modulates its density.
- [20] For a review, see e.g. R. Rajaraman, *Solitons and Instantons* (North-Holland, Amsterdam, 1982).
- [21] M. S. Foster, E. A. Yuzbashyan, and B. L. Altshuler, in preparation.